Available online at www.sciencedirect.com
ScienceDirect
Trans. Nonferrous Met. Soc. China 24(2014) 2824−2830
Transactions of Nonferrous Metals Society of China
www.tnmsc.cn

Effect of silicon content on microstructure of Al−Si/SiC_p composite layer cladded on A380 Al alloy by TIG welding process

Behnam LOTFI, Mehdi ROSTAMI, Zohreh SADEGHIAN

Department of Materials Science and Engineering, Faculty of Engineering, Shahid Chamran University, Ahvaz, Iran

Received 9 October 2013; accepted 21 January 2014

Abstract: Tungsten inert gas (TIG) welding was applied to creating a composite layer on the surface of cast aluminum alloy A380. Different mixtures of Al, Si and SiC powders mixed with sodium silicate solution were pasted on substrates. Surface melting was conducted by TIG welding to produce Al−SiC layer on the surface. Microstructural evolution was investigated by X-ray diffractometry (XRD), optical and scanning electron microscopy (SEM) and elemental microanalysis (EDS). Properties of clad layers were studied by microhardness and sliding wear testing. The results showed a uniform distribution of SiC particles in dendritic aluminum matrix. Addition of excess silicon caused the formation of eutectic crystals and coarse silicon particles in the clad layer which resulted in higher hardness and wear resistance of clad layers.

Key words: Al−SiC; TIG welding; composite clad layer; wear resistance

1 Introduction

Aluminum and its alloys are widely used in automotive, aerospace and petrochemical manufacturing industries due to attractive properties like high specific strength, excellent corrosion resistance and low density [1,2]. Despite excellent properties, application of these alloys is restricted because of their relatively poor wear resistance [3].

Different technologies such as anodizing, physical vapor deposition and electroplating have been used to create a thin hard layer on the surface and improve the wear behavior of the substrate [1,4,5]. These coatings are usually thin and may break up against applied forces. Thus, different methods of welding have been applied to creating a thick layer with good adhesion to the substrate [6−9]. Tungsten inert gas (TIG) welding is a promising process, which can produce a clad layer on the surface to enhance the surface hardness and wear resistance [10]. By the addition of strengthening particles like SiC, TiC and Al_2O_3, a composite clad layer can be created on aluminum substrate leading to higher hardness, wear resistance and thermal stability [11]. MAN and KOWOK [12] applied a composite layer containing SiC particles on 6061 Al alloy using laser cladding process. According to their X-ray diffractometry results, laser surface melting and creation of composite layers resulted in the formation of Al_4C_3 and Al_4SiC_4 phases and the hardness was increased consequently by 7 times. ANANDKUMAR et al [13] reported that increasing the input heat during laser cladding of Al−Si/$SiC_{(p)}$ composite coatings on cast aluminum 356 substrate caused a reaction between SiC particles and molten aluminum, which resulted in the formation of Al_4SiC_4 and Si particles in the composite layer and increased the hardness to HV270 [13].

In the present study, a composite clad layer containing a mixture of aluminum and silicon carbide powders was applied on the surface of cast aluminum substrate by TIG welding process. The effect of silicon addition on microstructure, hardness and wear resistance of the clad layer was investigated.

2 Experimental

Cast aluminum alloy A380 with a composition of Al−8.5Si−3.5Cu was used as substrate material. Surface area and thickness of the substrates were 30 mm× 100 mm and 10 mm, respectively. Al, SiC and Si powders were employed as the constituents of cladding material. Al powder had a particle size range of 20−40 μm

Corresponding author: Behnam LOTFI; Tel: +98-6113330010-5727; Fax: +98-6113336642; E-mail: behnaml@scu.ac.ir
DOI: 10.1016/S1003-6326(14)63414-2

with 99% purity, the size range of SiC particles was 25−35 μm with 99.5% purity, and Si powder had an average particle size of 25 mm with 99.9% purity. To achieve a uniform distribution of SiC particles in aluminium matrix, mixtures of Al and SiC with or without excess Si addition were milled for 30 min by a planetary ball mill. Mass ratio of ball to powder and rotating speed were 6 and 100 r/min, respectively. Hardfacing was performed in two stages. Firstly, the samples were polished and cleaned with acetone to remove the surface oxide layer and contaminations. The substrates were afterwards, covered by a paste, which was a mixture of 5 g pre-milled powder with 2 g of 20% sodium silicate aqua solution. The paste was applied on the surface with a spatula to provide a uniform thickness of 1 mm. Different powder mixture compositions were applied on the samples (Table 1). Coated samples were then dried in a furnace at 50 °C for 60 min. Tungsten inert gas (TIG) welding equipment schematically shown in Fig. 1, was utilized for surface melting process. Welding electrode was 2% thoriated tungsten and the shielding gas was argon (99.99% purity) with 8 mL/min flow rate. The current was alternative type (AC) with a square wave. Process parameters are given in Table 2 and Eq. (1) was used to estimate the input heating, in which V, I and S are voltage, current and welding speed, respectively. η, arc efficiency coefficient, which varies from 50% to 35%, was considered to be 48%.

$$E = \frac{\eta VI}{S} \quad (1)$$

Table 1 Different compositions of powder mixtures applied on aluminum substrate

Sample	w(SiC)/%	w(Al)/%	w(Si)/%
Al−20SiC	0	20	Bal.
Al−30SiC	0	30	Bal.
Al−20SiC−7.2Si	7.2	20	Bal.
Al−20SiC−12Si	12	20	Bal.

Table 2 TIG welding process parameters

I/A	V/V	Electrode	Input heating/(kJ·cm^{-1})
140	10	EWTh (2.4 mm)	67

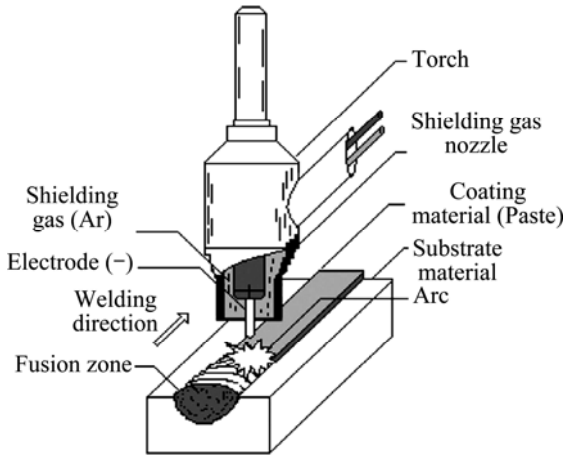

Fig. 1 Schematic illustration of cladding by TIG welding process

Transverse sections of cladded specimens were prepared, polished, and etched with Keller's solution (2 mL HF, 3 mL HCl, 5 mL HNO_3, 190 mL distilled water). Microstructural investigations were conducted by a Meiji Techno optical microscope. The cross-sectional microstructures together with spot analysis were studied with the aid of a LEO 1455 VP scanning electron microscope (SEM) equipped with an energy dispersive X-ray spectrometer (EDX). X-ray diffractometry with 1.542 Å Cu K_α and a step size of 0.02° between 20° to 90° was used to study the structural evolution of clad layers. Microhardness measurements with a load of 0.98 N (100 g) and duration of 15 s were carried out on cladded samples using Bowers Metrology Vickers digital microhardness machine.

Wear tests were performed by a pin-on disc apparatus, TRM 250 manual tribometer, under dry conditions and a normal load of 16 N at room temperature and each wear test was conducted using a fresh disc. Pin height losses were automatically measured by the machine at different intervals of wear distance. Cylindrical pin specimens of 6 mm in diameter and 33 mm in height were prepared from the clad layers by an electrode-discharge wire cutter. Pins were prepared with 1200 grade silicon carbide paper and held against a counterface (disc) which rotated in a horizontal plane. AISI E 52100 (Fe−1.0%C, 1.4%Cr, 0.40%Mn, 0.2%Si, 0.05%S, 0.05%P) polished discs with a hardness of HRC 62 were used as the counterparts. Volume losses of the pins were determined from the obtained height losses after each 400 m sliding. The total sliding distance was 2050 m. Worn surfaces and wear debris were studied by scanning electron microscope.

3 Results and discussion

Figure 2 shows the SEM image and EDS microanalysis of Al−20 SiC clad layer. SEM image of the clad layer demonstrated a relatively uniform distribution of SiC particles in aluminum matrix. EDS microanalysis of the matrix showed the existence of some little amount of Si in Al matrix (Fig. 2(b)). X-ray diffractometry of Al−20SiC sample confirmed the presence of Al and SiC as shown in Fig. 3. SEM image of Al−30SiC clad layer presented in Fig. 4 demonstrates a distribution of a dark needle-like phase as well as SiC in Al matrix. EDS microanalysis indicates that the

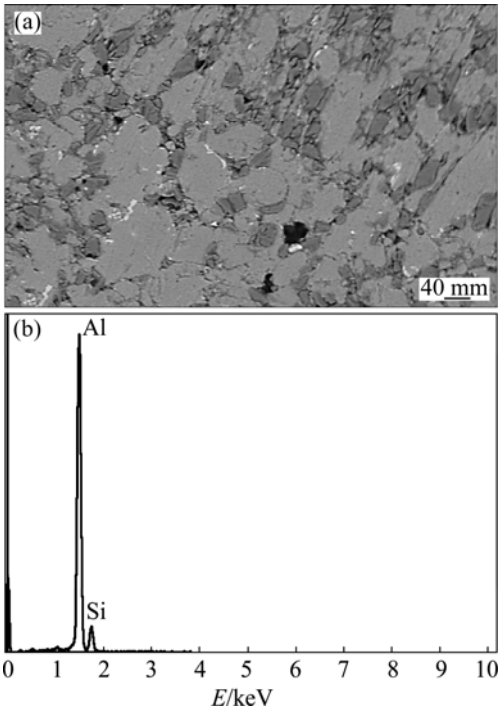

Fig. 2 Cross-sectional SEM image (a) and EDS microanalysis (b) of matrix of Al−20SiC clad layer

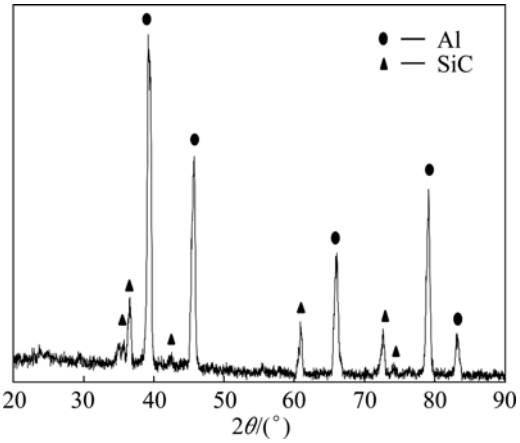

Fig. 3 XRD pattern of Al−20SiC clad layer applied on aluminum alloy substrate

needle-like phase consists of Al, Si, C and O (Fig. 4(b)). According to the previous studies on Al/SiC composite [13,14], this phase has been suggested to be Al_4SiC_4. The formation of this ternary carbide is attributed to a reaction between molten Al and SiC which might have occurred at TIG conditions by the following reaction [13]:

$$4Al(l)+3SiC(s)\rightarrow Al_4SiC_4(s)+3Si(s) \quad (2)$$

The formation of Al_4SiC_4 ternary carbide has been reported by other investigators to occur at temperatures above 1670 K and Al_4C_3 if formed in such conditions tends to this ternary carbide by a reaction with

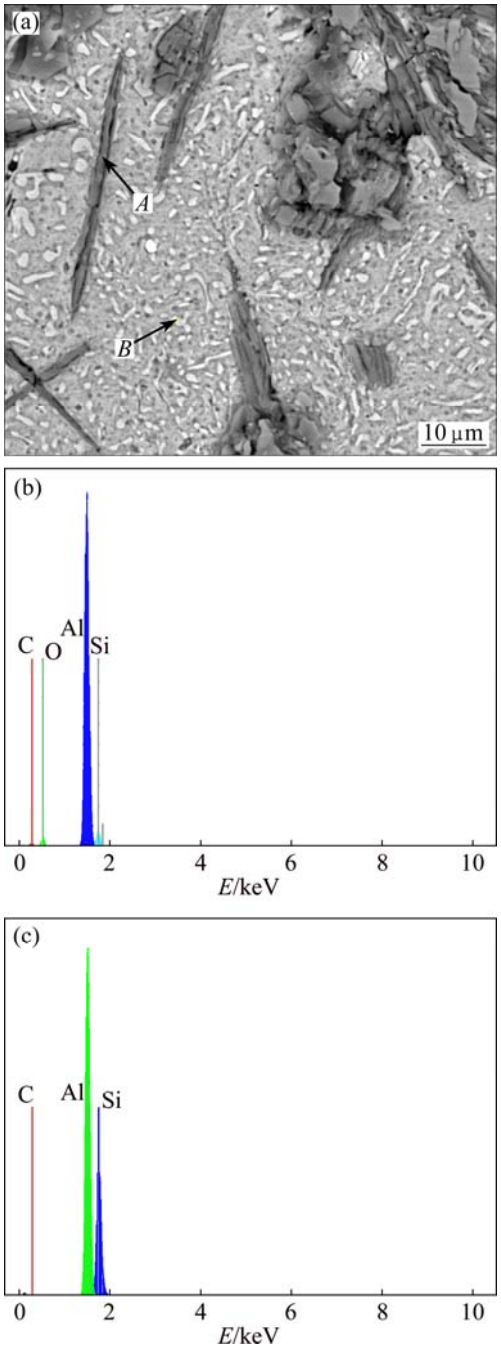

Fig. 4 Cross-sectional SEM image (a), EDS microanalysis of point *A* (b) and point *B* (c) of Al−30 SiC clad layer

SiC [15,16]. The resultant Si dissolved in molten Al. Si has a low solubility in solid Al according to Al−Si phase diagram; as a result, the Si-rich liquid solidifies to a eutectic structure containing acicular Si in Al matrix [17]. EDS microanalysis of the Al−30SiC composite clad layer (Fig. 4(c)) indicates the presence of Al and Si in the matrix which confirms the eutectic Al−Si structure. Similar results have been reported by ANANDKUMAR et al during laser cladding of Al−Si/SiC composite coatings [13].

As presented in Fig. 5, Al−30SiC exhibits a lower coherency to the substrate in comparison with Al−20SiC, which can be attributed to the existence of needle-like Al_4SiC_4 phase.

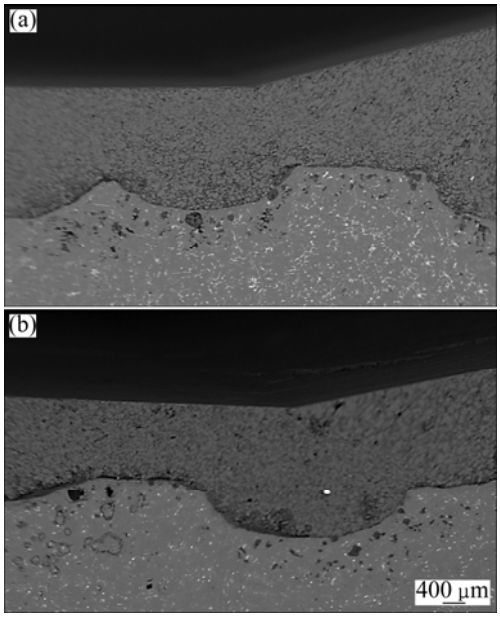

Fig. 5 Cross-sectional SEM images of Al−20SiC (a) and Al−30SiC (b) clad layers applied on aluminum alloy substrate

In order to increase the wettability of SiC particles in molten aluminum and to improve the clad layer adhesion to the substrate during the welding process, Si was added to the powder mixture according to Table 1. Figure 6 shows the optical microscopy image of Al−20SiC−7.2Si clad layer. Eutectic acicular Si crystals can be seen within the matrix. Eutectic Si crystals have been reported to germinate from the surface of SiC particles with an epitaxial structure [18]. As the Al−Si matrix solidifies, primary aluminum nucleates and grows in a dendritic structure. Therefore, the clad layer consists of ductile primary Al phase and brittle eutectic Si phase at room temperature [19].

Figure 7(a) shows the SEM image of Al−20SiC−12Si clad layer. Angular particles are formed with a bright gray contrast beside the SiC particles in Al matrix,

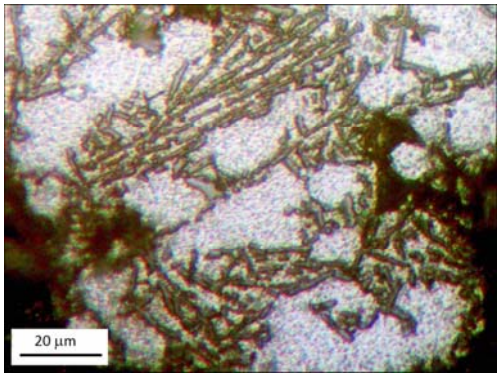

Fig. 6 Optical micrograph of Al−20SiC−7.2Si clad layer

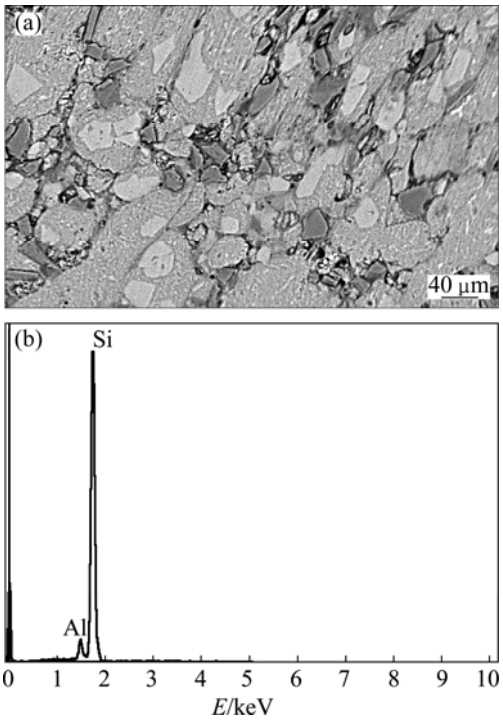

Fig. 7 SEM image (a) and EDS microanalysis (b) of selected point of Al−20SiC−12Si clad layer

which are revealed to be proeutectic Si by EDS microanalysis (Fig. 7(b)).

Figure 8 presents the X-ray diffraction patterns of the Al−20SiC−7.2Si and Al−20SiC−12Si samples. By increasing the Si amount in initial powder mixture, the intensity of Si peak increases. This is explained by the formation of proeutectic angular Si particles in Al−20SiC−12Si clad layer.

Table 3 presents the results of microhardness testing on clad layers. Surface hardness shows a good increase with the addition of SiC particles to about HV 130 in Al−30SiC clad layer compared with HV 70 of substrate material. This can be attributed to the formation of Al−Si eutectic structure together with hard, needle-shaped Al_4SiC_4 with a hardness of HV 400.

Moreover, adding excess Si content to initial powder mixture increases the surface hardness of Al−20SiC clad layer, which is due to the formation of eutectic Si in the matrix. Additional Si up to 12% in initial powder mixture has substantially increased the surface hardness (HV 190). This is because of the present of proeutectic Si particle with a hardness of about HV 400−800. ANANDKUMAR et al [13] reported the surface hardness of Al−Si/SiC_p composite laser clad layer to be about HV 140.

Volume losses of different clad layers and the substrate are presented in Fig. 9 as a function of sliding distance. Clad layers exhibited much lower volume loss

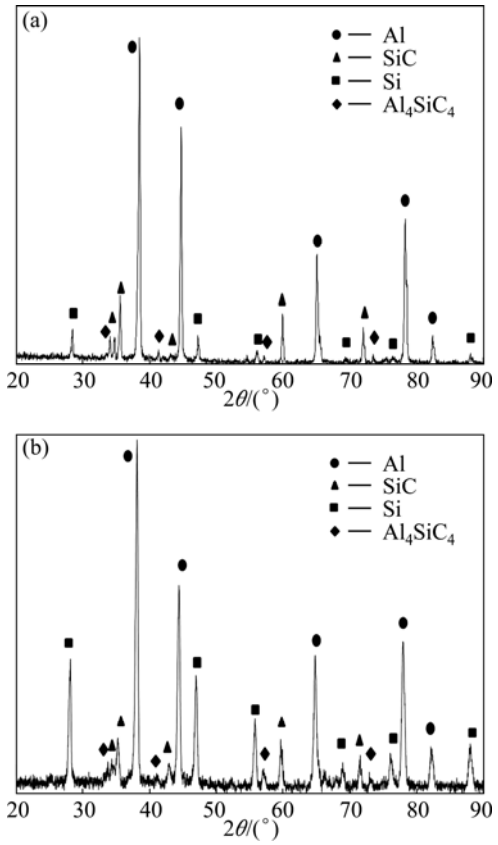

Fig. 8 XRD patterns of Al−20SiC−7.2Si (a) and Al−20SiC−12Si (b) clad layers

Table 3 Surface hardness of clad composites

Substrate	Al−20SiC	Al−30SiC	Al−20SiC−7.2Si	Al−20SiC−12Si
HV 70	HV 105	HV 132	HV 121	HV 190

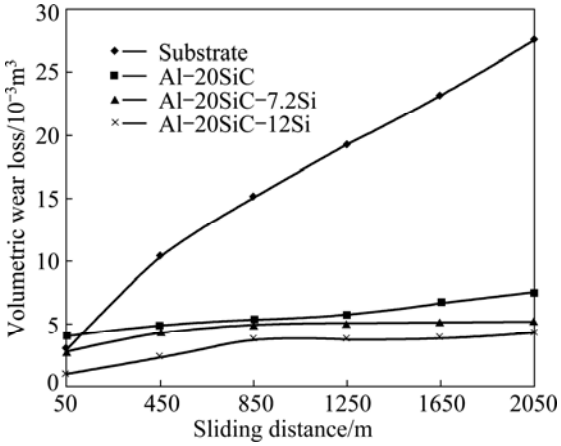

Fig. 9 Volume loss of different clad layers and substrate as function of sliding distance

compared with the substrate and this difference was increased by increasing sliding distance. It is clear that the substrate has a higher wear rate than all coatings. The existence of SiC particles leads to higher load capacity and protection of the surface against sliding wear scratches. The effect of SiC content on wear behavior of Al−SiC composites has been investigated previously [20−23]. Adding Si which resulted in the formation of acicular and block Si within the matrix increased the hardness and wear resistance of clad layers. Hard Si particles resist against destructive action during sliding and protect the surface against severe plastic deformation [24].

Figure 10 shows the SEM images of worn surfaces of substrate, Al−20SiC and Al−20SiC−7.2Si clad layers. On the substrate worn surface, overlapped layers

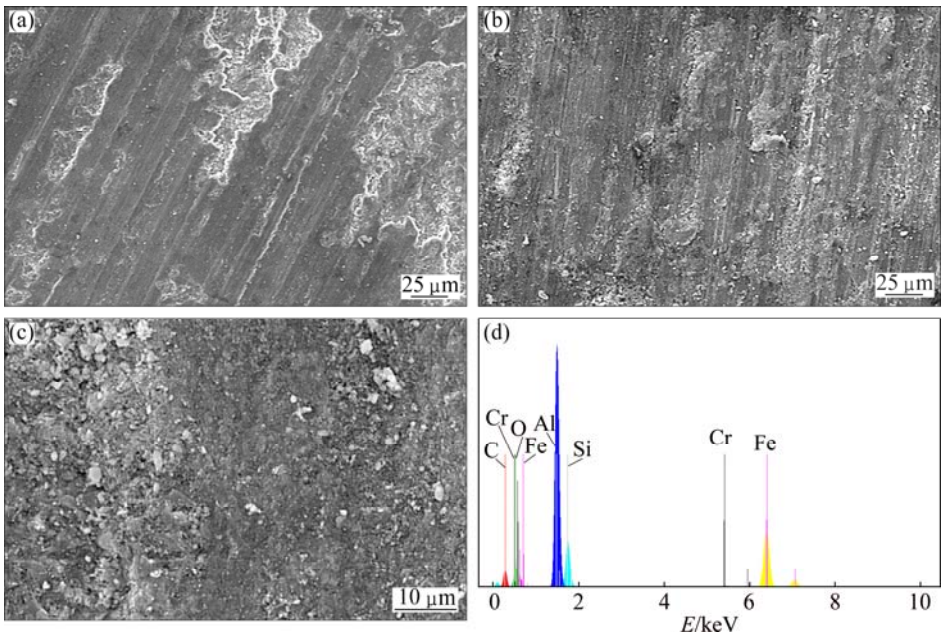

Fig. 10 SEM images of worn surfaces substrate (a), Al−20SiC (b) and Al−20SiC−7.2Si (c) clad layers and EDS analysis (d) of dark areas in Fig. 10(c)

together with micro ploughing are obvious. This can be contributed to severe plastic deformation during sliding and is a typical characteristic of delamination wear mechanism. The ploughing-grooves on worn surfaces are much shallower and finer in clad layers compared with the substrate. Several investigators have reported the predominant wear mechanism of Al alloys to be a combination of abrasive wear and delamination at low sliding speeds [24−26]. EDS microanalysis of dark areas on Al−20SiC−7.2Si clad layer (Fig. 10(c)) reveals high O and Fe contents, demonstrating an iron oxide transferred layer from sliding pin to the worn surface.

4 Conclusions

A composite clad layer containing SiC particles in Al−Si eutectic matrix was obtained by TIG welding process. Addition of 30% SiC, resulted in the formation of needle-shaped Al_4SiC_4 and a fine distribution of acicular silicon within the matrix. Addition of 7.2% or 12% silicon to the initial powder mixture caused the formation of eutectic crystals and coarse silicon particles in the clad layer. Hardness increased by increasing the quantity of SiC particles and silicon within the initial powder mixture. The highest surface hardness and sliding wear resistance were obtained in Al−20SiC−12Si clad layer.

References

[1] MALACZYNSKI G W, HAMDI A H, ELMOUSRI A A, QIU X. Ion implantation and diamond-like coatings of aluminum alloys [J]. Journal of Materials Engineering Performance, 1997, 6(2): 223−239.

[2] HEFTI L D. Commercial airplane applications of superplastically formed AA5083 aluminum sheet [J]. Journal of Materials Engineering Performance, 2007, 16(2): 136−141.

[3] HEFTI L D. ASM metals handbook, surface engineering [M]. Ohio: ASM International, 1993.

[4] LUGSCHEIDER E, KRÄMER G, BARIMANI C, ZIMMERMANN H. PVD coatings on aluminium substrates [J]. Surface and Coatings Technology, 1995, 74−75(1): 497−502.

[5] WANG A, FAN C, XIE C, HUANG W, CUI K. Laser cladding of iron-base alloy on Al−Si alloy and its relation to cracking at the interface [J]. Journal of Materials Engineering Performance, 1996, 5(6): 775−783.

[6] XU J, LIU W. Microstructure and wear properties of laser cladding Ti−Al−Fe−B coatings on AA2024 aluminum alloy [J]. Materials Design, 2006, 27: 405−410.

[7] SUN R, LEI Y. Microstructure and hardness of laser clad SiC_p−Al composite coatings on Al alloys [J]. Materials Letters, 2008, 62: 3272−3275.

[8] JENDRZEJEWSKI R, van ACKER K. Metal matrix composite production by means of laser dispersing of SiC and WC powder in Al alloy [J]. Applied Surface Science, 2009, 255: 5584−5587.

[9] YANG S, CHEN N. In situ formation of $MoSi_2$/SiC composite coating on pure Al by laser cladding [J]. Materials Letters, 2003, 57: 3412−3416.

[10] TOYSERKANI E, KHAJEPOUR A. Laser cladding [M]. Boca Raton, FL: CRC Press, 2005.

[11] STRAFFORD K N. Surface engineering practice: Processes fundamentals and applications in corrosion and wear [M]. Hertfordshire, UK: Ellis Horwood Limited, 1990.

[12] MAN H, KOWOK C. Cavitation erosion and corrosion behavior of laser surface alloyed MMC of SiC and Si_3N_4 on Al alloy AA6061 [J]. Surface and Coatings Technology, 2000, 132: 11−20.

[13] ANANDKUMAR R, ALMEDIA A, COLACO R, VILAR R, OCELIK V, HOSSON J T M. Microstructure and wear studies of laser clad Al−Si/$SiC_{(p)}$ composite coatings [J]. Surface and Coatings Technology, 2007, 201: 9497−9505.

[14] SIMCHI A, GODLINSKI D. Effect of SiC particles on the laser sintering of Al−7Si−0.3Mg alloy [J]. Scripta Materialia, 2008, 59: 199−202.

[15] WALTER D, KARAYASA I W. Solid state reactions in the Al−Si−C system [J]. Journal of the Chinese Chemical Society, 2005, 52: 873−876.

[16] UREŇA A, RODRIGO P, GIL L. Interfacial reactions in an Al−Cu−Mg (2009)/SiC_w composite during liquid processing [J]. Journal of Materials Science, 2001, 36: 429−439.

[17] CUI C, SCHULZ A, SCHIMANSKI K, ZOCH H W. Spray forming of hypereutectic Al−Si alloys [J]. Journal of Materials Processing and Technology, 2009, 209: 5220−5228.

[18] ROBLES F, SOKOLOWSKI J. Thermal analysis and microscopical characterization of Al−Si hypereutectic alloys [J]. Journal of Alloys and Compounds, 2006, 419: 180−190.

[19] YE E. An overview of the development of Al−Si−Alloy based material for engine applications [J]. Journal of Materials Engineering Performance, 2003, 12: 288−297.

[20] ŞAHIN Y. Abrasive wear behaviour of SiC/2014 aluminium composite [J]. Tribology International, 2010, 43: 939−943.

[21] MA T, YAMAURA H. Dry sliding wear behavior of cast SiC-reinforced Al MMCs [J]. Materials Science and Engineering A, 2003, 360: 116−125.

[22] RUBAIE K S, YOSHIMURA H N, MELLO J D B. Two-body abrasive wear of Al−SiC composites [J]. Wear, 1999, 233−235: 444−454.

[23] RUBAIE K S, GOLDENSTEIN H, MELLO J D B. Three-body abrasion of Al−SiC composites [J]. Wear, 1999, 225−229: 163−173.

[24] CHEN Zhen-hua, TENG Jie, CHEN Gang, FU Ding-fa, YAN Hong-ge. Effect of the silicon content and thermomechanical treatment on the dry sliding wear behavior of spray-deposited Al-Si/SiC_p composites [J]. Wear, 2007, 262: 362−368.

[25] XU G, KUTSUNA M, LIU Z, YAMADA K. Comparison between diode laser and TIG cladding of Co-based alloys on the SUS403 stainless steel [J]. Surface and Coating Technology, 2006, 201: 1138−1144.

[26] KWOK J, LIM S. High-speed tribological properties of some Al/SiC_p composites [J]. Composites Science and Technology, 1999, 59: 65−75.

硅含量对 TIG 焊 Al−Si/SiC$_p$ 复合层包覆 A380 铝合金显微组织的影响

Behnam LOTFI, Mehdi ROSTAMI, Zohreh SADEGHIAN

Department of Materials Science and Engineering, Faculty of Engineering,
Shahid Chamran University, Ahvaz, Iran

摘　要：采用钨极惰性气体(TIG)在铸态 A380 铝合金表面制备复合涂层。将 Al，Si 和 SiC 粉末混合物与硅酸钠溶液混合后涂覆在基材上，采用 TIG 焊进行表面熔化，在基体表面制备 Al−SiC 涂层。采用 XRD、SEM 和 EDS 研究显微组织的变化，采用显微硬度和滑动磨损试验研究包覆层的性能。结果表明，SiC 粒子均匀分布在树枝状的铝基体中。加入过量的硅造成包覆层共晶和粗大硅粒子的形成，从而导致包覆层具有较高的硬度和耐磨性。

关键词：Al−SiC：TIG 焊；复合包覆层；耐磨性

(Edited by Xiang-qun LI)